

RESEARCH ARTICLE

Phase diagram and transport properties of Sb-doped $\text{Ca}_{0.88}\text{La}_{0.12}\text{Fe}_2\text{As}_2$ single crystals

Xiang-Zhuo Xing¹, Wei Zhou¹, Chun-Qiang Xu², Nan Zhou¹, Fei-Fei Yuan¹,
Yu-Feng Zhang¹, Xiao-Feng Xu^{2,*}, Zhi-Xiang Shi^{1,†}

¹Department of Physics and Key Laboratory of MEMS of the Ministry of Education,
Southeast University, Nanjing 211189, China

²Department of Physics and Hangzhou Key Laboratory of Quantum Matters,
Hangzhou Normal University, Hangzhou 310036, China

Corresponding authors. E-mail: *xiaofeng.xu@hznu.edu.cn, †zxshi@seu.edu.cn

Received July 2, 2016; accepted August 26, 2016

The effects of isovalent Sb substitution on the superconducting properties of the $\text{Ca}_{0.88}\text{La}_{0.12}\text{Fe}_2(\text{As}_{1-y}\text{Sb}_y)_2$ system have been studied through electrical resistivity measurements. It is seen that the antiferromagnetic or structural transition is suppressed with Sb content, and a high- T_c superconducting phase, accompanied by a low- T_c phase, emerges at $0.02 \leq y \leq 0.06$. In this intermediate-doping regime, normal-state transport shows non-Fermi-liquid-like behaviors with nearly T -linear resistivity above the high- T_c phase. With further Sb doping, this high- T_c phase abruptly vanishes for $y > 0.06$ and the conventional Fermi liquid is restored, while the low- T_c phase remains robust against Sb impurities. The coincidence of the high- T_c phase and non-Fermi liquid transport behaviors in the intermediate Sb-doping regime suggests that AFM fluctuations play an important role in the observed non-Fermi liquid behaviors, which may be intimately related to the unusual nonbulk high- T_c phase in this system.

Keywords Sb doped $\text{Ca}_{0.88}\text{La}_{0.12}\text{Fe}_2\text{As}_2$ superconductors, electrical resistivity measurement, phase diagram

PACS numbers 74.62.Dh, 74.25.F-, 74.70.Xa

1 Introduction

A wide range of iron-based superconductors (IBSs) have been reported [1–4] ever since the discovery of superconductivity at 26 K in $\text{LaFeAs}(\text{O},\text{F})$ [5]. The parent compounds of IBSs usually undergo structure and spin-density-wave (SDW) transitions, while superconductivity often arises when chemical doping [1, 2, 6–10] or external pressure [11–14] are applied to suppress these SDW order or structure transitions. Remarkably, isovalent substitution is widely used in the chemical doping study, owing to its advantage that no extra carriers are introduced to the band; therefore, the electronic structure is nearly unchanged. For example, among IBSs, BaFe_2As_2 can be substituted with Ru [6] on the Fe site or with P on the As site [7–9], Sb or P are often used to substitute for As in 1111 systems [10, 15], and Pd is doped in Pt sites in the platinum-based superconductor SrPt_3P [16]. Moreover, co-doping techniques have been

proved to be an effective way to enhance the superconductivity [17–21]. Kudo *et al.* [22] have demonstrated that co-doping of La and P in the CaFe_2As_2 system can significantly enhance the bulk superconductivity up to 45 K by tuning the lattice parameters and the number of charge carriers. Very recently, the T_c of the newly discovered $\text{Ca}_{1-x}\text{La}_x\text{FeAs}_2$ (112-type) superconductors has been boosted to 47 K by La and Sb co-doping [23].

Among IBSs, much attention has been paid to studying the physical properties of 122-type superconductors owing to their available high-quality single crystals with appreciable sizes. CaFe_2As_2 is a typical parent compound of AeFe_2As_2 (Ae=alkaline earth, 122-type) superconductors, which exhibits an AFM ordering at $T_N = 170$ K that is concomitant with a structural transition from tetragonal phase to orthorhombic phase at ambient pressure [24]. Moreover, the tetragonal phase will transform to a collapsed tetragonal (CT) phase upon applying external pressure [25, 26] or doping the rare-earth (Pr or Nd) into the parent compound [24–27]. Superconductiv-

ity can be induced by electron- or hole-doping on the Ca site [28–32], transition-metal (Co, Ni) doping on the Fe site [33, 34], isovalent substitution on the As site [9], or applying external pressure [11, 35]. Distinct from other 122-type IBSs, superconductivity with two successive superconducting transitions (high- T_c phase and low- T_c phase) has been observed in this system by rare earth doping or applied pressure [27, 36, 37]. The high- T_c phase reaches as high as 42–49 K and is believed to be *nonbulk* in origin, since the diamagnetic signal is so sensitive to the applied magnetization field and no zero resistance is observed [31]. However, the mechanism of this unusual *nonbulk* high- T_c superconductivity is still controversial, which has been attributed to a minor foreign phase, interface, or filamentary superconductivity in this system [31, 38–40].

To our knowledge, there have been no reports in the literature regarding the isovalent substitution of Sb for As in 122-type IBSs. In this paper, we report the synthesis of new Sb-doped superconductors, $\text{Ca}_{0.88}\text{La}_{0.12}\text{Fe}_2(\text{As}_{1-y}\text{Sb}_y)_2$. We study the effects of La and Sb co-doping on the superconducting properties of this system and construct the phase diagram through electrical resistivity measurements. It is found that the high- T_c phase is closely related to the non-Fermi liquid behaviors, which in turn may be correlated with the AFM fluctuations. Our results, therefore, provide more insight into the underlying origin of the unusual *nonbulk* high- T_c superconductivity in the (Ca,La)Fe₂As₂ system.

2 Experiments

Single crystals of $\text{Ca}_{0.88}\text{La}_{0.12}\text{Fe}_2(\text{As}_{1-y}\text{Sb}_y)_2$ were grown from FeAs flux as previously reported [36, 37]. The FeAs precursor was first synthesized by reacting a stoichiometric amount of Fe powder with As chips at 1065°C or 10 h in a vacuum quartz tube. Stoichiometric mixtures of Ca:La:FeAs:Fe:Sb=0.88:0.12:4(1-y):4y:4y were placed in an alumina crucible and sealed in an evacuated quartz tube. The samples were heated to 1180°C slowly and held for 10 h before slowly cooling down to 960°C to grow the single crystals. Plate-like single crystals were harvested mechanically from the flux. Single crystal and powder X-ray diffraction (XRD) measurements were performed using a Rigaku diffractometer with Cu K α radiation. The resistivity was measured using the standard four-probe method on a Physical Property Measurement System (Quantum Design).

3 Results and discussion

Figure 1 shows the single crystal XRD patterns of $\text{Ca}_{0.88}\text{La}_{0.12}\text{Fe}_2(\text{As}_{1-y}\text{Sb}_y)_2$ with various Sb-doping lev-

els. Only (00 l) peaks are observed, indicating good c -axis orientation of the samples. The lattice parameters as a function of y are shown as the inset of Fig. 1, the lattice parameters c were also obtained by fitting the powder XRD data (not shown). We find that the lattice parameters remain almost unchanged with doping, the strange origin may come from the interaction between the Ca/La atoms and the As/Sb atoms, similar to the results of the Sr and Sb co-doped PrFeAsO system [19]. In addition, we notice that the c parameter is also hardly changed by isovalent doping of Sb in $\text{Ca}_{1-x}\text{La}_x\text{FeAs}_2$ (112-type) superconductor [23]. The actual La content is close to the nominal composition by EDX measurement, while the actual content of Sb could not be determined by EDX because of the substantial peak overlaps of Sb and Ca in EDX spectra [23], so the nominal values of Sb doping will be used in what follows. As we will show below, the suppression of AFM/structural transition, the variation of the high- T_c phase, as well as subtle changes in the normal state transport coefficients with doping *all* suggest that Sb atoms were indeed incorporated into the system.

Figure 2 presents the T -dependence of resistivity normalized to their respective 300 K values for the crystals used in this study. The resistivity anomaly associated with the SDW or structure transition shifts to lower temperatures and disappears around $y = 0.04$. Meanwhile, the high- T_c superconducting phase emerges at $y = 0.02$. Two superconducting transitions (high- T_c phase and low- T_c phase) can be observed up to $y = 0.06$. Extending to higher substitution levels ($y > 0.06$), the high- T_c phase vanishes abruptly and only the low- T_c phase persists. However, non-zero resistivity was observed for some doping levels, indicating a nonbulk superconducting character, in contrast to the La and P co-doping which can induce bulk superconductivity up to 45 K [22].

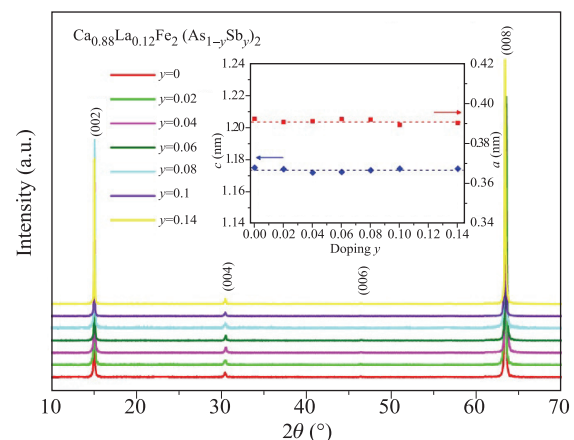


Fig. 1 The single-crystal X-ray diffraction patterns of $\text{Ca}_{0.88}\text{La}_{0.12}\text{Fe}_2(\text{As}_{1-y}\text{Sb}_y)_2$ for different doping y . Inset: The lattice parameters as a function of nominal Sb content y . The dashed lines are guides to the eye.

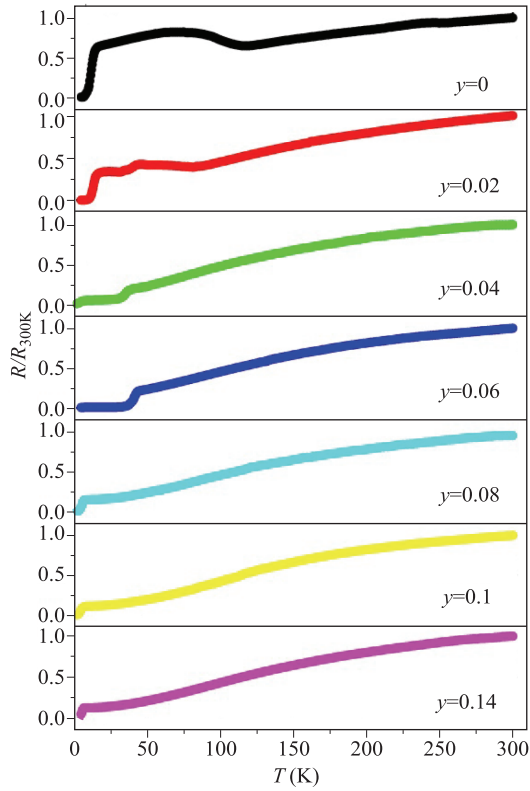


Fig. 2 T -dependence of the renormalized in-plane electrical resistivity for $\text{Ca}_{0.88}\text{La}_{0.12}\text{Fe}_2(\text{As}_{1-y}\text{Sb}_y)_2$ single crystals.

In order to check the influence of magnetic fields on the two superconducting phases, the electrical resistivity under different magnetic fields applied along the ab -plane and the c -axis are presented for $y = 0.04$ sample in Figs. 3(a) and (b), respectively. T_c is gradually suppressed and the transition is broadened by increasing the fields for both directions. However, the effect of fields applied along the c -axis is more sensitive to the field than along the ab -plane, which is a typical response to the field directions in the $(\text{Ca},\text{RE})\text{Fe}_2\text{As}_2$ system [32, 37, 41]. H_{c2} - T phase diagram obtained by 90% of normal state resistivity is plotted in Fig. 3(c). Two upper critical fields, corresponding to the high- T_c phase and the low- T_c phase respectively, are clearly observed. H_{c2} exhibits upward curvature near T_c for both the in-plane and out-of-plane directions, which has been commonly observed in this system [37].

Now, let us turn to the effects of Sb substitution on the normal state transport properties. The normal state resistivity follows a power-law behavior according to $\rho(T) = \rho_0 + AT^n$ in the range of $T_{c1}(T_{c2}) < T \leq 70$ K, where ρ_0 is the residual resistivity and A is a constant. Figures 4(a), (b), and (c) represent the fitting results using the power law as shown by red lines for some selected samples $y = 0.06, 0.08,$ and 0.14 . T -linear resistivity was

observed in $y = 0.06$, indicating a non-Fermi-liquid behavior, which usually occurs around a quantum critical point in iron-based superconductors [7, 8]. Upon further Sb doping, n increases to a value of 2, suggesting the restoration of the Fermi liquid (FL) ground state when $y > 0.06$. Similar T^2 resistivity was also observed in Ni- or P-doped CaFe_2As_2 single crystals [9, 34].

The resultant phase diagram of $\text{Ca}_{0.88}\text{La}_{0.12}\text{Fe}_2(\text{As}_{1-y}\text{Sb}_y)_2$ from the resistivity measurements has been constructed in Fig. 5. In this diagram, superconductivity coexists with the AFM/structural transition at low doping levels ($y \leq 0.02$). With increasing doping, the AFM/structural transition is suppressed and vanishes above $y > 0.02$. Meanwhile, a high- T_c superconducting phase emerges in the intermediate-doping region ($0.02 \leq y \leq 0.06$). In the high-doping regime, the high- T_c phase vanishes abruptly, in contrast to the sole rare earth (La, Ce, Pr, and Nd) doping in CaFe_2As_2 where the high T_c superconducting phase is hardly suppressed once it emerges [24, 27, 36]. In contrast, the low- T_c

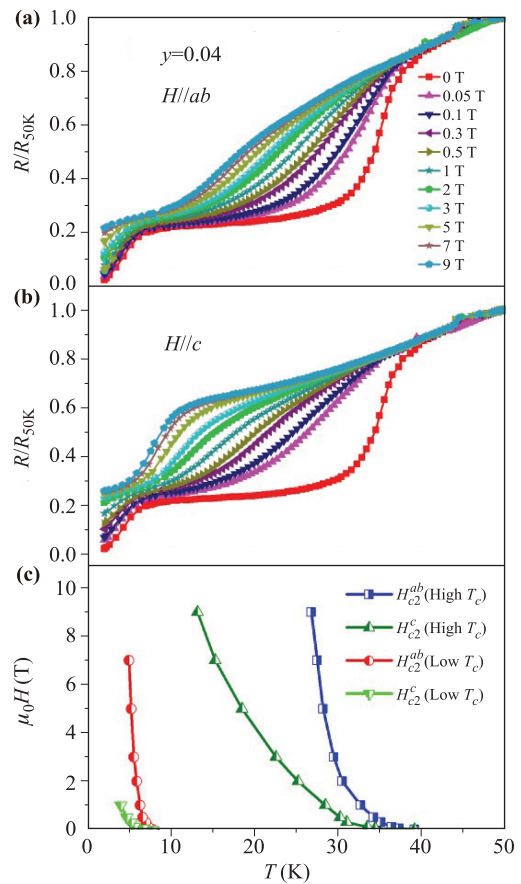


Fig. 3 T -dependence of the electrical resistivity for the field (a) parallel, and (b) perpendicular to the ab -plane under various applied fields for $y = 0.04$ sample. (c) T -dependence of H_{c2} extracted from the upper two panels.

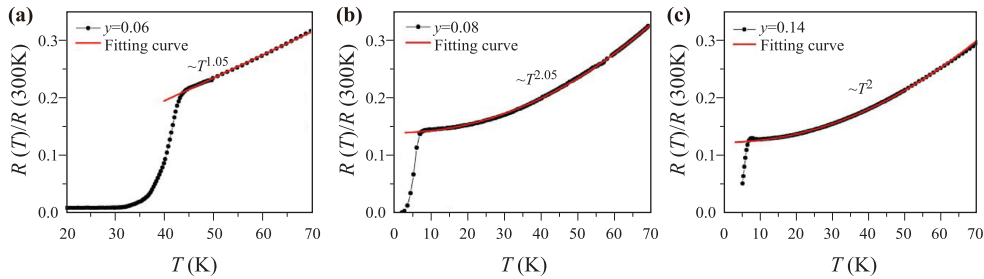


Fig. 4 Normal state transport for some typical samples with $y = 0.06$ (a), $y = 0.08$ (b) and $y = 0.14$ (c) at low temperatures, the red lines are fits to $\rho(T) = \rho_0 + AT^n$.

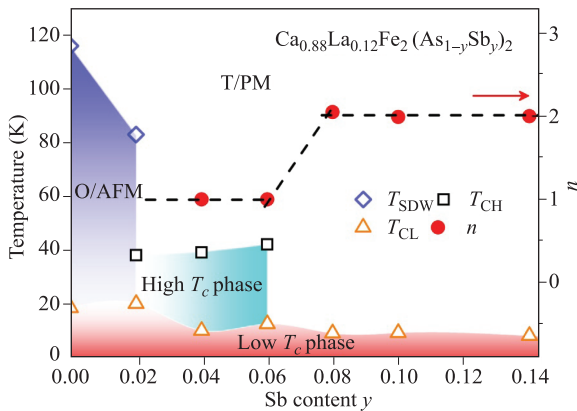


Fig. 5 The phase diagram of $\text{Ca}_{0.88}\text{La}_{0.12}\text{Fe}_2(\text{As}_{1-y}\text{Sb}_y)_2$ determined from the resistivity measurements, exponent n was obtained by fitting the power law $\rho(T) = \rho_0 + AT^n$.

phase, which is related to a strain-induced phase, as that of SrFe_2As_2 parent compound [42], remains robust against any Sb doping levels. On the other hand, it is noteworthy that the exponent n from the $\rho(T)$ fitting is closely related to the high- T_c phase in this system. In the intermediate regime where the high- T_c phase arises, the value of n is approximately equal to 1, whilst in the high doping levels, the high- T_c phase disappears and n amounts to 2. The concomitance between the high- T_c phase and the non-Fermi liquid signature suggests this high- T_c superconductivity be induced by the non-Fermi liquid excitations. Similar to many other quantum critical materials, the non-Fermi liquid behaviors in our system may come from the AFM fluctuations in the intermediate regime. These phenomena indicate that the AFM fluctuations may play an important role for the nonbulk high- T_c superconducting phase in the $(\text{Ca},\text{La})\text{Fe}_2\text{As}_2$ system. We also note that similar results were observed in $\text{CaFe}_2(\text{As}_{1-x}\text{P}_x)_2$ [9] across the tetragonal to collapsed tetragonal phase transition, which contributed to the reduction of interband nesting in the electronic structure.

4 Conclusion

In conclusion, Sb-doped $\text{Ca}_{0.88}\text{La}_{0.12}\text{Fe}_2(\text{As}_{1-y}\text{Sb}_y)_2$ superconductors have been successfully synthesized for the first time. We systematically studied the electrical transport properties and derived the phase diagram from resistivity measurements. A high- T_c superconducting phase, accompanied by T -linear resistivity in the normal state, was observed at $0.02 \leq y \leq 0.06$ when the AFM/structure transition was suppressed, but this phase vanished abruptly once $y > 0.06$, where the Fermi liquid transport recovers. The simultaneous disappearance of the high- T_c superconductivity and the non-Fermi liquid transport state suggests that the unusual nonbulk high- T_c superconducting phase may be closely related to the AFM fluctuations in the $(\text{Ca},\text{La})\text{Fe}_2\text{As}_2$ system.

Acknowledgements This work was supported by the National Natural Science Foundation of China (Grant Nos. U1432135, 11674054, 11474080, and 11611140101) and the Scientific Research Foundation of Graduate School of Southeast University (Grant No. YBJJ1621). X. Xu would also like to acknowledge the National Key Basic Research Program of China (Grant No. 2014CB648400) and the support from the Distinguished Young Scientist Funds of Zhejiang Province (No. LR14A040001).

References

1. H. H. Wen and S. L. Li, Materials and novel superconductivity in iron pnictide superconductors, *Annu. Rev. Condens. Matter Phys.* 2(1), 121 (2011)
2. M. Rotter, M. Tegel, and D. Johrendt, Superconductivity at 38 K in the iron arsenide $(\text{Ba}_{1-x}\text{K}_x)\text{Fe}_2\text{As}_2$, *Phys. Rev. Lett.* 101(10), 107006 (2008)
3. N. Ni, J. M. Allred, B. C. Chan, and R. J. Cava, High T_c electron doped $\text{Ca}_{10}(\text{Pt}_3\text{As}_8)(\text{Fe}_2\text{As}_2)_5$ and $\text{Ca}_{10}(\text{Pt}_4\text{As}_8)(\text{Fe}_2\text{As}_2)_5$ superconductors with skutterudite intermediary layers, *Proc. Natl. Acad. Sci. USA* 108(45), E1019 (2011)

4. N. Katayama, K. Kudo, S. Onari, T. Mizukami, K. Sugawara, Y. Sugiyama, Y. Kitahama, K. Iba, K. Fujimura, N. Nishimoto, M. Nohara, and H. Sawa, Superconductivity in $\text{Ca}_{1-x}\text{La}_x\text{FeAs}_2$: A novel 112-type iron pnictide with arsenic zigzag bonds, *J. Phys. Soc. Jpn.* 82(12), 123702 (2013)
5. Y. Kamihara, T. Watanabe, M. Hirano, and H. Hosono, Iron-based layered superconductor $\text{La}[\text{O}_{1-x}\text{F}_x]\text{FeAs}$ ($x = 0.05 - 0.12$) with $T_c = 26$ K, *J. Am. Chem. Soc.* 130(11), 3296 (2008)
6. M. J. Eom, S. W. Na, C. Hoch, R. K. Kremer, and J. S. Kim, Evolution of transport properties of $\text{BaFe}_{2-x}\text{Ru}_x\text{As}_2$ in a wide range of isovalent Ru substitution, *Phys. Rev. B* 85(2), 024536 (2012)
7. S. Kasahara, T. Shibauchi, K. Hashimoto, K. Ikada, S. Tonegawa, R. Okazaki, H. Shishido, H. Ikeda, H. Takeya, K. Hirata, T. Terashima, and Y. Matsuda, Evolution from non-Fermi- to Fermi-liquid transport via isovalent doping in $\text{BaFe}_2(\text{As}_{1-x}\text{P}_x)_2$ superconductors, *Phys. Rev. B* 81(18), 184519 (2010)
8. S. Jiang, H. Xing, G. Xuan, C. Wang, Z. Ren, C. Feng, J. Dai, Z. Xu, and G. Cao, Superconductivity up to 30 K in the vicinity of the quantum critical point in $\text{BaFe}_2(\text{As}_{1-x}\text{P}_x)_2$, *J. Phys.: Condens. Matter* 21(38), 382203 (2009)
9. S. Kasahara, T. Shibauchi, K. Hashimoto, Y. Nakai, H. Ikeda, T. Terashima, and Y. Matsuda, Abrupt recovery of Fermi-liquid transport following the collapse of the c axis in $\text{CaFe}_2(\text{As}_{1-x}\text{P}_x)_2$ single crystals, *Phys. Rev. B* 83(6), 060505(R) (2011)
10. C. Wang, S. Jiang, Q. Tao, Z. Ren, Y. Li, L. Li, C. Feng, J. Dai, G. Cao, and Z. A. Xu, Superconductivity in $\text{LaFeAs}_{1-x}\text{P}_x\text{O}$: Effect of chemical pressures and bond covalency, *Europhys. Lett.* 86(4), 47002 (2009)
11. M. S. Torikachvili, S. L. Bud'ko, N. Ni, and P. C. Canfield, Pressure induced superconductivity in CaFe_2As_2 , *Phys. Rev. Lett.* 101(5), 057006 (2008)
12. H. Takahashi, K. Igawa, K. Arii, Y. Kamihara, M. Hirano, and H. Hosono, Superconductivity at 43 K in an iron-based layered compound $\text{LaO}_{1-x}\text{F}_x\text{FeAs}$, *Nature* 453(7193), 376 (2008)
13. P. L. Alireza, Y. T. Ko, J. Gillett, C. M. Petrone, J. M. Cole, G. G. Lonzarich, and S. E. Sebastian, Superconductivity up to 29 K in SrFe_2As_2 and BaFe_2As_2 at high pressures, *J. Phys.: Condens. Matter* 21(1), 012208 (2009)
14. L. Sun, X. J. Chen, J. Guo, P. Gao, Q. Z. Huang, H. Wang, M. Fang, X. Chen, G. Chen, Q. Wu, C. Zhang, D. Gu, X. Dong, L. Wang, K. Yang, A. Li, X. Dai, H. K. Mao, and Z. Zhao, Re-emerging superconductivity at 48 K in iron chalcogenides, *Nature* 483(7387), 67 (2012)
15. S. J. E. Carlsson, F. Levy-Bertrand, C. Marcenat, A. Sulpice, J. Marcus, S. Pairis, T. Klein, M. Núñez-Regueiro, G. Garbarino, T. Hansen, V. Nassif, and P. Toulemonde, Effect of the isoelectronic substitution of Sb for As on the magnetic and structural properties of $\text{LaFe}(\text{As}_{1-x}\text{Sb}_x)\text{O}$, *Phys. Rev. B* 84(10), 104523 (2011)
16. K. K. Hu, B. Gao, Q. C. Ji, Y. H. Ma, H. Zhang, G. Mu, F. Q. Huang, C. B. Cai, and X. M. Xie, Impurity scattering effect in Pd-doped superconductor SrPt_3P , *Front. Phys.* 11(4), 117403 (2016)
17. J. Prakash, S. J. Singh, G. Thakur, S. Patnaik, and A. K. Ganguli, The effect of antimony doping on the transport and magnetic properties of $\text{Ce}(\text{O}/\text{F})\text{FeAs}$, *Supercond. Sci. Technol.* 24(12), 125008 (2011)
18. S. J. Singh, J. Prakash, S. Patnaik, and A. K. Ganguli, Enhancement of the superconducting transition temperature and upper critical field of $\text{LaO}_{0.8}\text{F}_{0.2}\text{FeAs}$ with antimony doping, *Supercond. Sci. Technol.* 22(4), 045017 (2009)
19. Q. Ji, B. Gao, G. Mu, T. Hu, W. Li, Y. Liu, Y. Ma, and X. Xie, Enhancement of superconductivity by Sb-doping in the hole-doped iron-pnictide superconductor $\text{Pr}_{1-x}\text{Sr}_x\text{FeAsO}$, *Physica C* 498, 50 (2014)
20. X. Xing, W. Zhou, B. Xu, N. Li, Y. Sun, Y. Zhang, and Z. Shi, Co-co-doping effect on superconducting properties of 112-type $\text{Ca}_{0.8}\text{La}_{0.2}\text{FeAs}_2$ single crystals, *J. Phys. Soc. Jpn.* 84(7), 075001 (2015)
21. H. Yakita, H. Ogino, A. Sala, T. Okada, A. Yamamoto, K. Kishio, A. Iyo, H. Eisaki, and J. Shimoyama, Co and Mn doping effect in polycrystalline (Ca,La) and $(\text{Ca},\text{Pr})\text{FeAs}_2$ superconductors, *Supercond. Sci. Technol.* 28(6), 065001 (2015)
22. K. Kudo, K. Iba, M. Takasuga, Y. Kitahama, J. Matsumura, M. Danura, Y. Nogami, and M. Nohara, Emergence of superconductivity at 45 K by lanthanum and phosphorus co-doping of CaFe_2As_2 , *Sci. Rep.* 3, 1478 (2013)
23. K. Kudo, Y. Kitahama, K. Fujimura, T. Mizukami, H. Ota, and M. Nohara, Superconducting transition temperatures of up to 47 K from simultaneous rare-earth element and antimony doping of 112-type CaFeAs_2 , *J. Phys. Soc. Jpn.* 83(9), 093705 (2014)
24. S. R. Saha, N. P. Butch, T. Drye, J. Magill, S. Ziemak, K. Kirshenbaum, P. Y. Zavalij, J. W. Lynn, and J. Paglione, Structural collapse and superconductivity in rare-earth-doped CaFe_2As_2 , *Phys. Rev. B* 85(2), 024525 (2012)
25. A. Kreyssig, M. A. Green, Y. Lee, G. D. Samolyuk, P. Zajdel, J. W. Lynn, S. L. Bud'ko, M. S. Torikachvili, N. Ni, S. Nandi, J. B. Leão, S. J. Poulton, D. N. Argyriou, B. N. Harmon, R. J. McQueeney, P. C. Canfield, and A. I. Goldman, Pressure-induced volume-collapsed tetragonal phase of CaFe_2As_2 as seen via neutron scattering, *Phys. Rev. B* 78(18), 184517 (2008)
26. A. I. Goldman, A. Kreyssig, K. Prokeš, D. K. Pratt, D. N. Argyriou, J. W. Lynn, S. Nandi, S. A. J. Kimber, Y. Chen, Y. B. Lee, G. Samolyuk, J. B. Leão, S. J. Poulton, S. L. Bud'ko, N. Ni, P. C. Canfield, B. N. Harmon, and R. J. McQueeney, Lattice collapse and quenching of magnetism in CaFe_2As_2 under pressure: A single-crystal neutron and X-ray diffraction investigation, *Phys. Rev. B* 79(2), 024513 (2009)

27. B. Gao, X. Li, Q. Ji, G. Mu, W. Li, T. Hu, A. Li, and X. Xie, Phase diagram and weak-link behavior in Nd-doped CaFe_2As_2 , *New J. Phys.* 16(11), 113024 (2014)
28. K. Zhao, Q. Q. Liu, X. C. Wang, Z. Deng, Y. X. Lv, J. L. Zhu, F. Y. Li, and C. Q. Jin, Doping dependence of the superconductivity of $(\text{Ca}_{1-x}\text{Na}_x)\text{Fe}_2\text{As}_2$, *Phys. Rev. B* 84(18), 184534 (2011)
29. J. J. Ying, J. C. Liang, X. G. Luo, X. F. Wang, Y. J. Yan, M. Zhang, A. F. Wang, Z. J. Xiang, G. J. Ye, P. Cheng, and X. H. Chen, Transport and magnetic properties of La-doped CaFe_2As_2 , *Phys. Rev. B* 85(14), 144514 (2012)
30. D. M. Wang, X. C. Shangguan, J. B. He, L. X. Zhao, Y. J. Long, P. P. Wang, and L. Wang, Superconductivity at 35.5 K in K-doped CaFe_2As_2 , *J. Supercond. Nov. Magn.* 26(6), 2121 (2013)
31. B. Lv, L. Deng, M. Gooch, F. Wei, Y. Sun, J. K. Meen, Y. Y. Xue, B. Lorenz, and C. W. Chu, Unusual superconducting state at 49 K in electron-doped CaFe_2As_2 at ambient pressure, *Proc. Natl. Acad. Sci. USA* 108(38), 15705 (2011)
32. Z. Gao, Y. Qi, L. Wang, D. Wang, X. Zhang, C. Yao, C. Wang, and Y. Ma, Synthesis and properties of La-doped CaFe_2As_2 single crystals with $T_c = 42.7$ K, *Europhys. Lett.* 95(6), 67002 (2011)
33. L. Harnagea, S. Singh, G. Friemel, N. Leps, D. Bombor, M. Abdel-Hafiez, A. U. B. Wolter, C. Hess, R. Klingeler, G. Behr, S. Wurmehl, and B. Büchner, Phase diagram of the iron arsenide superconductors $\text{Ca}(\text{Fe}_{1-x}\text{Co}_x)_2\text{As}_2$ ($0 \leq x \leq 0.2$), *Phys. Rev. B* 83(9), 094523 (2011)
34. N. Kumar, S. Chi, Y. Chen, K. Rana, A. Nigam, A. Thamizhavel, W. Ratcliff, S. Dhar, and J. Lynn, Evolution of the bulk properties, structure, magnetic order, and superconductivity with Ni doping in $\text{CaFe}_{2-x}\text{Ni}_x\text{As}_2$, *Phys. Rev. B* 80(14), 144524 (2009)
35. M. Torikachvili, S. Bud'ko, N. Ni, P. Canfield, and S. Hannahs, Effect of pressure on transport and magnetotransport properties in CaFe_2As_2 single crystals, *Phys. Rev. B* 80(1), 014521 (2009)
36. Y. Sun, W. Zhou, L. J. Cui, J. C. Zhuang, Y. Ding, F. F. Yuan, J. Bai, and Z. X. Shi, Evidence of two superconducting phases in $\text{Ca}_{1-x}\text{La}_x\text{Fe}_2\text{As}_2$, *AIP Adv.* 3(10), 102120 (2013)
37. W. Zhou, F. F. Yuan, J. C. Zhuang, Y. Sun, Y. Ding, L. J. Cui, J. Bai, and Z. X. Shi, Upper critical fields and anisotropy of $\text{Ca}_{1-x}\text{La}_x\text{Fe}_2\text{As}_2$ single crystals, *Supercond. Sci. Technol.* 26(9), 095003 (2013)
38. K. Gofryk, M. Pan, C. Cantoni, B. Saparov, J. E. Mitchell, and A. S. Sefat, Local inhomogeneity and filamentary superconductivity in Pr-doped CaFe_2As_2 , *Phys. Rev. Lett.* 112(4), 047005 (2014)
39. I. Zeljkovic, D. Huang, C.L. Song, B. Lv, C.W. Chu, and J. E. Hoffman, Nanoscale surface element identification and dopant homogeneity in the high- T_c superconductor $\text{Pr}_x\text{Ca}_{1-x}\text{Fe}_2\text{As}_2$, *Phys. Rev. B* 87, 201108(R) (2013)
40. L. Z. Deng, B. Lv, K. Zhao, F. Y. Wei, Y. Y. Xue, Z. Wu, and C. W. Chu, Evidence for defect-induced superconductivity up to 49 K in $(\text{Ca}_{1-x}\text{R}_x)\text{Fe}_2\text{As}_2$, *Phys. Rev. B* 93(5), 054513 (2016)
41. Y. Qi, Z. Gao, L. Wang, D. Wang, X. Zhang, C. Yao, C. Wang, C. Wang, and Y. Ma, Transport properties and anisotropy in rare-earth doped CaFe_2As_2 single crystals with T_c above 40 K, *Supercond. Sci. Technol.* 25(4), 045007 (2012)
42. S. R. Saha, T. Drye, S. K. Goh, L. E. Klintberg, J. M. Silver, F. M. Grosche, M. Sutherland, T. J. S. Munsee, G. M. Luke, D. K. Pratt, J. W. Lynn, and J. Paglione, Segregation of antiferromagnetism and high-temperature superconductivity in $\text{Ca}_{1-x}\text{La}_x\text{Fe}_2\text{As}_2$, *Phys. Rev. B* 89(13), 134516 (2014)